ChemComm

Accepted Manuscript

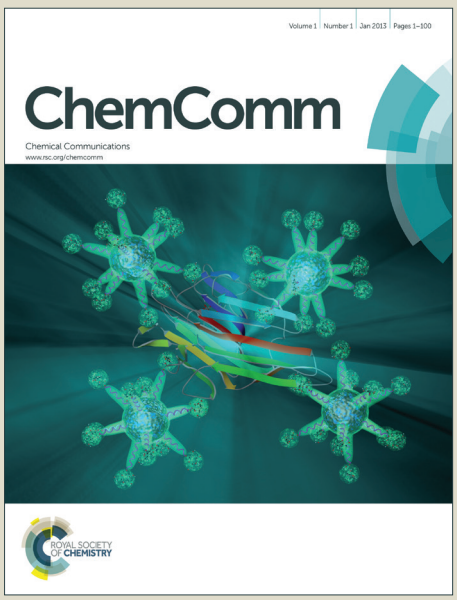

ROYAL SOCIETY OF CHEMISTRY

www.rsc.org/chemcomm

Cite this: DOI: 10.1039/c0xx00000x

www.rsc.org/chemcomm

COMMUNICATION

COSAN as a molecular imaging platform: Synthesis and "*in vivo*" imaging.

Kiran B. Gona,[a] Adnana Zaulet,[b] Vanessa Gómez-Vallejo,[a] Francesc Teixidor,[b] Jordi Llop[a,*] and Clara Viñas[b,*]

Received (in XXX, XXX) Xth XXXXXXXXX 20XX, Accepted Xth XXXXXXXXX 20XX
DOI: 10.1039/b000000x

A labelling method for the covalent attachment of radioiodine to the boron-rich 8-I-cobaltabisdicarbollide (I-COSAN) and a bi-functional (iodine and PEG) COSAN derivative, [3,3'-Co(8-I-1,2-$C_2B_9H_{10}$)(8'-$(OCH_2CH_2)_2COOC_6H_5$-1',2'-$C_2B_9H_{10}$ is reported. Biodistribution studies in rodents using dissection/gamma counting and *in vivo* nuclear imaging have been performed. The general strategy reported here can be applied in the future to COSAN derivatives bearing a wide range of functionalities.

Abnormal metabolism and over-expression of membrane receptors in cancer cells have been historically exploited to deliver therapeutic amounts of boron into tumours using boronated carbohydrate,[1] amino acid, peptide,[2] and nucleic acid derivatives,[3] and immunoconjugates.[4] With the emergence of nanotechnology, drug delivery systems such as liposomes, which may passively accumulate in the tumour thanks to enhanced permeability and retention (EPR) effect, have gained attention.[5]

The inorganic, boron-based molecule cobaltabisdicarbollide, [3,3'-Co(1,2-$C_2B_9H_{11}$)$_2$]$^-$, commonly known as COSAN (Figure 1), is a stable complex in which the cobalt atom is sandwiched between two η^5-bonding $[C_2B_9H_{11}]^{2-}$ moieties.[6] While showing differentiated properties from lipid molecules (e.g. amphiphilic character in water),[7] COSAN has the ability to assemble into monolayer vesicles.[8] As recently demonstrated by us, COSAN can cross through synthetic lipid membranes without disrupting membrane integrity[9] and accumulates *in vitro* within living cells.[10] Additionally, it can be readily multi-decorated by incorporation of functional groups in the different vertexes. These properties, together with its high boron content, its chemical stability and its solubility in physiologic conditions,[6] turn COSAN into a suitable building block for the preparation of boron carrier drugs.

Despite the large variety of COSAN derivatives described in the literature with potential application in boron neutron capture therapy (BNCT), the transition from bench to bed (even in the preclinical setting) has been only occasionally approached. The main reason behind this fact still remains the lack of techniques able to determine, *in vivo* and on real time, the accumulation of boron in the tumour and surrounding tissue, allowing a candidate-by-candidate screening and prediction of therapeutic efficacy. Nuclear imaging techniques such as Positron Emission Tomography (PET) and Single Photon Emission Computerized Tomography (SPECT) in combination with X-ray Computed Tomography (CT) are valuable tools for the *in vivo* assessment of pharmacokinetic properties of new chemical entities;[11] they are thus anticipated to be suitable methods for determining boron accumulation in the tumour and surrounding tissues. Nonetheless, application of nuclear imaging requires radiolabelling of the molecule under investigation with a positron or gamma emitter.[12] To date and to the best of our knowledge, radiolabelling of polyhedral boranes and heteroboranes with the radionuclide covalently attached to the cluster cage has been restricted to *nido* and *closo* derivatives.[13]

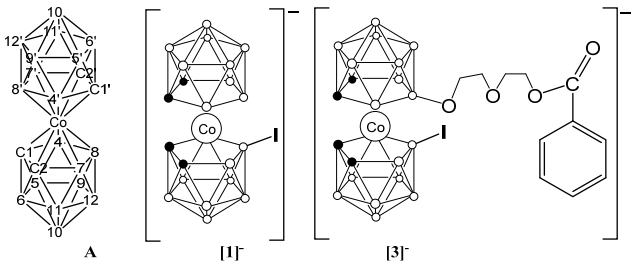

Figure 1.- Vertex numbering of anionic COSAN cluster (A) and their iodinated derivatives [3,3'-Co(8-I-1,2-$C_2B_9H_{10}$)(1',2'-$C_2B_9H_{11}$)]$^-$, [**1**]$^-$, and [3,3'-Co(8-I-1,2-$C_2B_9H_{10}$)(8'-$(OCH_2CH_2)_2COOC_6H_5$-1',2'-$C_2B_9H_{10}$)]$^-$, [**3**]$^-$, respectively.

In this paper, the synthesis of a new bi-functional (iodine and polyethylene glycol, PEG) COSAN derivative and its unprecedented radiolabelling with either ^{125}I (gamma emitter) or ^{124}I (positron emitter) *via* palladium catalyzed isotopic exchange reaction are reported. Incorporation of ^{125}I and ^{124}I enabled the determination of the biodistribution pattern by using dissection/gamma counting and PET-CT, respectively. Comparison with its parent I-COSAN, [3,3'-Co(8-I-1,2-$C_2B_9H_{10}$)(1',2'-$C_2B_9H_{11}$)]$^-$, was also carried out. The general strategy reported here should be suitable for the radiolabelling of specifically targeted COSAN derivatives, enabling their evaluation *in vivo* and facilitating translation into the clinical setting.

First, and with the aim of generating mixed-doubly functionalized COSAN derivatives simultaneously incorporating two markedly different reactive sites (i.e. a PEG branch and a suitable moiety for subsequent incorporation of the radioisotope), the synthesis of [3,3'-Co(8-I-1,2-$C_2B_9H_{10}$)(8'-$(OCH_2CH_2)_2COOC_6H_5$-1',2'-

$C_2B_9H_{11})]^-$, [**3**]$^-$, was carried out (Scheme 1). In brief, to a solution of 225 mg (0.39 mmol) of Na[3,3'-Co(8-$(OCH_2CH_2)_2COOC_6H_5$-1,2-$C_2B_9H_{11}$)(1,2-$C_2B_9H_{11}$)], Na[**2**],[14] in 10 mL of reagent grade CH_2Cl_2, 200 mg of iodine (0.78 mmol) were added. The reaction mixture was left to stand overnight at room temperature and then heated under reflux for 1.5h. The excess iodine was quenched with aqueous Na_2SO_3 solution, the resulting mixture was evaporated, and the orange solid was washed with water before been extracted with diethyl ether (3x10mL). After drying over anhydrous $MgSO_4$, the organic layer was evaporated to obtain Na[**3**] in 81% yield.

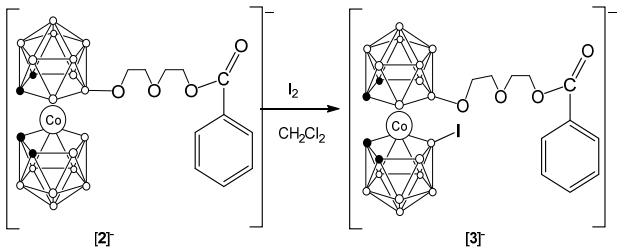

Scheme 1.- Synthesis of mixed doubly functionalized derivative of COSAN.

The MALDI-TOF analysis showed the desired molecular peak at 659.28 m/z corresponding to M (100%) and a fragmentation peak at 553.26 (M-I, 6%). The IR showed bands at 3040, 2947-2869, 2568-2539, 1736 and 1100-1071 cm^{-1} corresponding to C_c-H, C_{alkyl}-H, B-H, C-O and O-C-O, respectively.

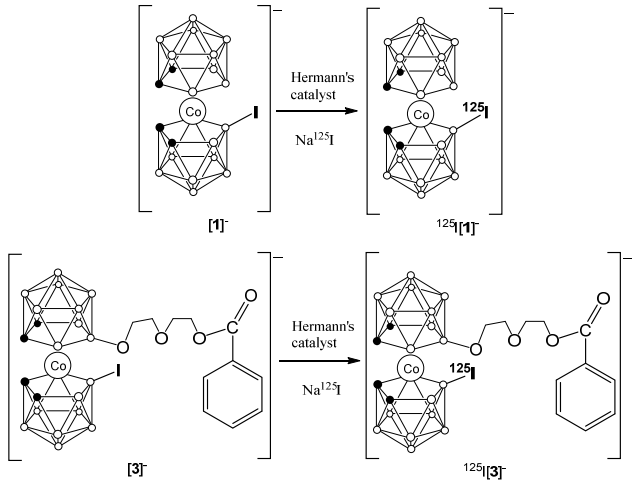

Scheme 2.- Radioiodination reaction of mono anionic species ^{125}I-[**1**]$^-$ (top) and ^{125}I-[**3**]$^-$ (bottom). Reaction conditions for [**1**]$^-$: Na[^{125}I]I, Hermann's catalyst, Toluene, 100°C, 3 min. Reaction conditions for [**3**]$^-$: Na[^{125}I]I, Hermann's catalyst, Toluene, 80°C, 8 min.

Radiolabelling reactions on compounds [**1**]$^-$ and [**3**]$^-$ were performed by adapting the previously reported palladium catalyzed iodine exchange reaction on iodinated dicarba-*closo*-dodecaborane.[13b] Experimental conditions were first optimized using ^{125}I, which is a convenient radioisotope due to its long half-life (59.4 d) and low cost. With that aim, the precursor ([**1**]$^-$ and [**3**]$^-$, 2.6 µmol) was reacted with 740 KBq (20 µCi) of Na[^{125}I]I (solution in 0.1M aqueous NaOH) in the presence of Hermann's catalyst (0.1mg) (Scheme 2). Radiochemical conversion values close to 85% were achieved for compound [**1**]$^-$ when the reaction was conducted at 100°C for 3 min, as determined by high performance liquid chromatography (HPLC) using radiometric detection; longer reaction times did not improve radiochemical conversion. For compound [**3**]$^-$, the formation of unidentified labelled species was detected when the reaction was conducted at 100°C. Lower reaction temperatures (80ºC) led to almost 80% radiochemical conversion after 8 min. Again, longer reaction times yielded lower incorporation yields, suggesting the degradation of the precursor and the radiolabelled compound. Purification by semi-preparative HPLC followed by solvent evaporation and reconstitution with C_2H_5OH/H_2O (1/9) resulted in injectable solutions of chemically and radiochemically pure compounds (see Figure S1 for example of chromatographic profile).

Lipophilicity of the radiolabelled compounds was calculated by the distribution coefficient (LogD). LogD values of 1.1±0.1 and 1.5±0.1 were obtained for ^{125}I-[**1**]$^-$ and ^{125}I-[**3**]$^-$, respectively. These results indicate that the presence of the PEG arm in [**3**]$^-$ results in a slight increase in the lipophylicity.

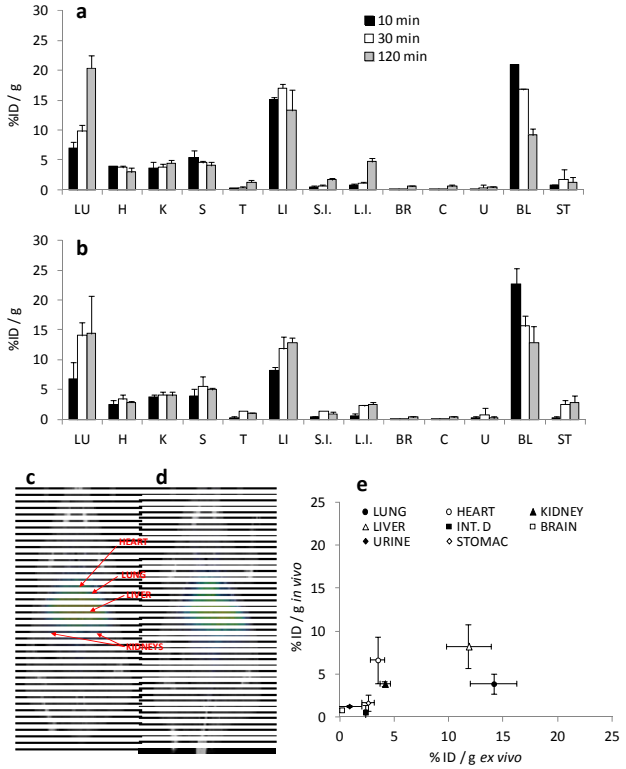

Figure 2.- Biodistribution of ^{125}I-[**1**]$^-$ (a) and ^{125}I-[**3**]$^-$ (b) in mice tissues (mean ± standard deviation, n=3) using the dissection method. Radioactivity is expressed as the percentage of the injected dose (ID) per gram of tissue. LU: Lungs; H: Heart; K: Kidneys; S: Spleen; T: Testicles; L: Liver; S.I.: Small intestine; L.I.: Large intestine; BR: Brain; C: Cerebellum; U: Urine; BL: Blood; ST: Stomach; (c-d) PET coronal projections resulting from averaged images (frames 12-20) obtained after administration of ^{124}I-[**1**]$^-$ (c) and ^{124}I-[**3**]$^-$ (d). Co-registration with CT images of the same animal is shown; (e) correlation between results obtained using PET-CT (expressed as %ID/cm^3 of tissue) and dissection and gamma counting (expressed as %ID/g of tissue) for compound ^{125}I-[**3**]$^-$ at 30 minutes after administration.

Biodistribution studies using dissection and gamma counting were performed in mice. The amount of radioactivity in the different organs was determined at three time points after

administration of the radiolabelled species (10, 30 and 120 minutes, Figures 2a, 2b).

Very similar patterns were obtained for both compounds: high accumulation in liver throughout the duration of the study, increasing uptake in the lungs and moderate blood clearance. Uptake in the kidneys and the spleen was also significant and lower accumulation was detected in other organs. Progressive accumulation in the intestine and the low concentration of radioactivity in the bladder (urine) suggest biliary excretion.

Moving towards *in vivo* application, the incorporation of the positron emitter ^{124}I was approached; with that aim, the radiolabelling process was performed following the optimized experimental conditions developed for ^{125}I, with equivalent incorporation ratios.

In vivo PET studies were conducted in combination with CT (Figure 2c, 2d), the latter for anatomical localization of the volumes of interest (VOIs). PET acquisitions were started concomitantly with the administration of the radiolabelled ^{124}I-[**1**]$^-$ and ^{124}I-[**3**]$^-$ species, and dynamic images were acquired (20 frames, total acquisition time of 130 min). In this case, only those organs clearly visualized on the CT images (lung, heart, kidney, liver, intestine, brain, bladder and stomach) were analyzed (Figures S2 and S3). Good correlation between results obtained using both methodologies (*in vivo* imaging and dissection/gamma counting) were obtained (Figures 2e and S4), although significant differences were observed at different time points in the brain, the bladder and the lungs. As a general trend, higher accumulation values in the brain were obtained *in vivo*, probably due to the contribution of the blood to the overall quantification of the uptake in this region. In the particular case of the lungs, the differences can be attributed to the fact that the percentage of injected dose (%ID) per gram of tissue is measured *ex vivo*, whereas *in vivo*, the %ID per cm^3 is obtained. Because the density of the lungs significantly differs from 1g/cm^3, the results obtained in both experiments cannot be directly compared. Differences observed in the bladder might be due to urination during image acquisition (*in vivo*) or uptake time (*ex vivo*). Interestingly, *in vivo* studies did not show accumulation of radioactivity in the thyroid gland, suggesting the stability of both ^{124}I-[**1**]$^-$ and ^{124}I-[**3**].

Conclusions

A new bifunctional COSAN derivative incorporating a PEG arm and one iodine atom has been synthesized and successfully radiolabelled with ^{124}I and ^{125}I via palladium catalyzed iodine exchange. The biodistribution pattern of the radiolabelled cobaltabisdicarbollide species has been determined using dissection/gamma counting and real-time, *in vivo* and noninvasive imaging (PET-CT). The general radiolabelling strategy reported here, which can be applied in the future to COSAN derivatives bearing a wide range of functionalities, might be applicable to targeted cobaltabisdicarbollides able to selectively accumulate in tumors. Hence, our method may become an invaluable, widely applied tool for the fast and accurate evaluation of new COSAN-based BNCT drug candidates in animal tumor models. Due to the noninvasive nature of PET imaging, potential translation into the clinical setting to predict therapeutic efficacy in a patient-by-patient basis can be also foreseen.

Notes and references

[a] Radiochemistry and Nuclear Imaging, CIC biomaGUNE, Paseo de Miramón 182, 20009 Donostia - San Sebastian, Spain.
E-mail: jllop@cicbiomagune.es; Fax: +34 94 3005301
[b] Institut de Ciència de Materials de Barcelona (ICMAB-CSIC),Campus de la U.A.B., E-08193 Bellaterra, Spain.
E-mail: clara@icmab.es; Fax: +34 93 5805729

‡ This work was supported by Generalitat de Catalunya (2009/SGR/00279), and Spanish Ministry of Economy and Competitiveness (CTQ2010-16237). A. Z. is is enrolled in the PhD program of the UAB. The authors would like to thank Maria Puigivila for assisstance in experimental work involving animals and Zuriñe Baz for image analysis.

§ The animals were maintained and handled in accordance with the Guidelines for Accommodation and Care of Animals (European Convention for the Protection of Vertebrate Animals Used for Experimental and Other Scientific Purposes) and internal guidelines. Experimental procedures were approved by local authorities.

1 (a) S. Ronchi, D. Prosperi, C. Thimon, C. Morin and L. Panza, *Tetrahedron Asymmet.*, 2005, **16**, 39; (b) S. Stadlbauer, P. Welzel and E. Hey-Hawkins, *Inorg. Chem.*, 2009, **48**, 5005, (c) S. Stadlbauer, P. Loennecke, P. Welzel and E. Hey-Hawkins, *Eur. J. Org. Chem.*, 2010, **16**, 3129.

2 (a) V. M. Ahrens, R. Frank, S. Stadbauer, A. G. Beck-Sickinger and E. Hey-Hawkins, *J. Med. Chem.*, 2011, **54**, 2368; (b) M. Yu. Stogniy, M. V. Zakharova, I. B. Sivaev, I. A. Godovikov, A. O. Chizov and V. I. Bregadze, *Polyhedron*, 2013, **55**, 117; (c) C. Morin and C. Thimon, *Eur. J. Org. Chem.*, 2004, **2004**, 3828.

3 (a) S. Hasabelnaby, A. Goudah, H. K. Agarwal, M. S.M. Abdalla and W. Tjarks, *Eur. J. Med. Chem.*, 2012, **55**, 325; (b) A. Semioshkin, A. Ilinova, I. Lobanova, V. Bregadze, E. Paradowska, M. Studzińska, A. Jabłońska and Z. J. Lesnikowski, *Tetrahedron*, 2013, **37**, 8034.

4 (a) W. Yang, R. F. Barth, G. Wu, W. Tjarks, P. Binns and K. Riley, *Appl. Radiat. Isot.*, 2009, **67(7-8)**, S328.

5 (a) K. Maruyama, O. Ishida, S. Kasaoka, T. Takizawa, N. Utoguchi, A. Shinohara, M. Chiba, H. Kobayashi, M. Eriguchi and H. J. Yanagie, *Control. Release*, 2004, **98**, 195; (b) H. Koganei, M. Ueno, S. Tachikawa, L. Tasaki, H. S. Ban, M. Suzuki, K. Shiraishi, K. Kawano, M. Yokoyama, Y. Maitani, K. Ono and H. Nakamura, *Bioconjugate Chem.*, 2013, **24**, 124; (c) S. Masunaga, S. Kasaoka, K. Maruyama, D. Nigg, Y. Sakurai, K. Nagata, M. Suzuki, Y. Kinashi, A. Maruhashi and K. Ono, *Int. J. Radiat. Oncol. Biol. Phys.*, 2006, **66**, 1515; (d) X. Pan, G. Wu, W. Yang, R. F. Barth, W. Tjarks and R. J. Lee, *Bioconjug. Chem.*, 2007, **18**, 101; (e) M. Ueno, H. S. Ban, K. Nakai, R. Inomata, Y. Kaneda, A. Matsumura and H. Nakamura, *Bioorg. Med. Chem.*, 2010, **18(9)**, 3059.

6 N. Grimes. *Carboranes*. Academic Press: Burlington, MA, 2011.

7 P. Matějíček, P. Cígler, K. Procházka and V. Král, *Langmuir*, 2006, **22**, 575.

8 P. Bauduin, S. Prevost, P. Farras, F. Teixidor, O. Diat and T. Zemb, *Angew. Chem. Int. Ed. Engl.*, 2011, **50**, 5298.

9 C. Verdiá-Báguena, A. Alcaraz, V. M. Aguilella, A. M. Cioran, S. Tachikawa, H. Nakamura, F. Teixidor and C. Viñas, *Chem. Commun.*, 2014, **50(51)**, 6677.

10 M. Tarrés, E. Canetta, C. Viñas, F. Teixidor and A. J. Harwood, *Chem. Commun.*, 2014, **50(51)**, 3370.

11 M. D. Bartholomä, A. S. Louie, J. F. Valliant and J. Zubieta, *Chem. Rev.* 2010, **110(5)**, 2903.

12 S. Achilefu, *Chem. Rev.*, 2010, **110(5)**, 2575.

13 (a) V. Tolmachev, A. Bruskin, I. Sivaev, H. Lundqvist and S. Sjöberg, *Radiochim. Acta*, 2002, **90**, 229; (b) K. J. Winberg, G. Barberà, L. Eriksson, F. Teixidor, V. Tolmachev, C. Viñas, and S. Sjöberg, *J. Organomet. Chem.*, 2003, **680**, 188; (c) D. S. Wilbur, D. K. Hamlin, R. R. Srivastava and M. K. Chyan, *Nucl. Med. Biol.*, 2004, **31**, 523; (d) M. E. El-Zaria, N. Janzen, M. Blacker and J. F. Valliant, *Chem. Eur. J.*, 2012, **18(35),** 11071. (e) K. B. Gona, V. Gómez-Vallejo, D. Padro and J. Llop, *Chem. Commun.*, 2013, **49**, 11491.

14 P. Farràs, F. Teixidor, R. Kivekäs, R. Sillanpää, C. Viñas, B. Grüner and I. Cisarova, *Inorg. Chem.*, 2008, **47(20)**, 9497.